An Electrode Array for Limiting Blood Loss During Liver Resection: Optimization *via* Mathematical Modeling

R.M. Strigel[1], D.J. Schutt[2], J.G. Webster[3], D.M. Mahvi[4] and D. Haemmerich*[,2,5]

[1]*Department of Surgery, University Wisconsin-Madison, USA*

[2]*Division of Pediatric Cardiology, Medical University of South Carolina, USA*

[3]*Department of Biomedical Engineering, University Wisconsin-Madison, USA*

[4]*Department of Surgery, Northwestern University, USA*

[5]*Department of Bioengineering, Clemson University, USA*

Abstract: Liver resection is the current standard treatment for patients with both primary and metastatic liver cancer. The principal causes of morbidity and mortality after liver resection are related to blood loss (typically between 0.5 and 1 L), especially in cases where transfusion is required. Blood transfusions have been correlated with decreased long-term survival, increased risk of perioperative mortality and complications. The goal of this study was to evaluate different designs of a radiofrequency (RF) electrode array for use during liver resection. The purpose of this electrode array is to coagulate a slice of tissue including large vessels before resecting along that plane, thereby significantly reducing blood loss. Finite Element Method models were created to evaluate monopolar and bipolar power application, needle and blade shaped electrodes, as well as different electrode distances. Electric current density, temperature distribution, and coagulation zone sizes were measured. The best performance was achieved with a design of blade shaped electrodes (5 × 0.1 mm cross section) spaced 1.5 cm apart. The electrodes have power applied in bipolar mode to two adjacent electrodes, then switched sequentially in short intervals between electrode pairs to rapidly heat the tissue slice. This device produces a ~1.5 cm wide coagulation zone, with temperatures over 97 ºC throughout the tissue slice within 3 min, and may facilitate coagulation of large vessels.

INTRODUCTION

Liver (or hepatic) resection (i.e. surgical removal of part of the liver containing a tumor) remains the primary treatment option for long-term disease-free survival in patients with metastatic colorectal cancer or primary liver cancer [1, 2]. In 2007, primary liver cancer was diagnosed in 19,100 patients in the United States and was responsible for 16,800 deaths. Further it is estimated that there were 153,800 new cases of colorectal cancer in the United States and 52,200 deaths [3]. Approximately 50 to 60% of patients with colorectal cancer will develop metastatic disease to the liver at some point during the course of their illness and of those patients 10 to 25% will be candidates for surgical resection [4]. The outcome of untreated liver cancer is poor, with a five-year survival rate of 0 to 1% [2]. Five-year survival rates following liver resection are between 27 and 43% [2].

The principal cause of morbidity and mortality after liver resection is related to intraoperative bleeding [5-7], which is due to the large number of highly perfused vessels that are present in the liver. Blood loss has been significantly reduced during the recent decades using a variety of techniques [5, 6, 8]. However, blood loss still remains a concern, with typical blood loss in recent studies of 425 mL to 1100 mL during liver resection [2, 8, 9]. Blood loss has been correlated to reduced patient survival, especially in cases of high blood loss where blood transfusion is required [6, 10-14]. Transfusions are still required in 18 to 47% of patients [2, 6, 10, 15-17], and cause complications likely due to immune system reactions. Patients requiring blood transfusion have a decreased long-term survival, increased risk of perioperative mortality, higher complication rate, longer length of hospital stay, and increased risk of infectious complications [17].

Tumor ablation techniques are currently used to locally treat cancer by heating the tumor by radiofrequency (RF) current or microwaves. Several groups suggested the use of ablation techniques for a different application - to assist with liver resection [7, 18-21]. Surgical resection is performed along a plane of healthy liver tissue, the so-called resection plane. Ablative techniques can assist in limiting blood loss by coagulating a slice of tissue in the resection plane (i.e. ablating healthy tissue, contrary to heating the tumor as performed during conventional tumor ablation), before cutting the tissue along that plane. This technique may also decrease tumor recurrence because by heating the resection plane, a sterile margin between the cancerous (to be removed) part of the liver, and healthy liver is created [7]. Current ablation devices for tumor ablation are optimized to create a spherical coagulation zone, 3-5 cm in diameter. Coagulating a slice of tissue therefore requires inserting, withdrawing, and reinserting a conventional ablation electrode multiple times to create a slice of coagulated tissue

*Address correspondence to this author at the Medical University of South Carolina, 165 Ashley Ave, MSC 915, Charleston, SC 29425, USA; Tel: (843) 792-1396; E-mail: haemmer@musc.edu

1874-1207/10

[7, 21]. This can be time consuming, with one study citing a mean of 30 radiofrequency applications, 4 min each for RF-assisted resection [18]. Nevertheless, this technique has the potential to limit interoperative blood loss to a minimum. Zhou *et al*. [7] compared microwave assisted liver resection with a control group and demonstrated that the microwave coagulation group experienced less blood loss and fewer transfusions. In a more recent study, Weber *et al*. [21] used RF assisted resection in 15 patients undergoing hepatic wedge resections (i.e. a wedge of liver is resected). They used RF needle electrodes employing multiple insertions and ablations to create a confluent slice of coagulated tissue, and achieved average blood loss of 30 mL; no blood transfusions were required.

We present a new device that consists of a linear array of electrodes (Fig. **1**), which are placed in the resection plane (see Fig. **3**) to coagulate this tissue plane. We use the finite element method (FEM) to investigate different electrode array designs, and electrode types (Fig. **2**). The electrode array is placed in the resection plane (Fig. **3**), and can potentially coagulate a 1-2 cm wide slice of tissue within ~3 min.

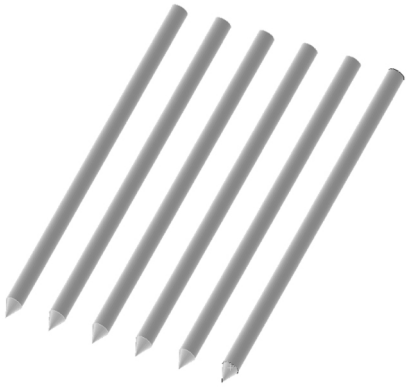

Fig. (1). Linear array of needle electrodes.

Fig. (2). Blade electrode with 5 × 0.1 mm cross section (left), and needle electrode with 1.2 mm (18 gauge) diameter (right), both 50 mm long.

MATERIALS AND METHODS

We investigated different designs to obtain a coagulation zone of 1-2 cm width throughout a slice of liver tissue. We determined this width to enable easy cutting along the coagulation zone without sacrificing too much healthy tissue. To ensure coagulation of large vessels, we attempted to obtain as high tissue temperatures as possible throughout the tissue slice. Current RF devices can only coagulate vessels that are close to the electrode, and up to a maximum of 3 mm in diameter [22]. We investigated arrays of both needle and blade shaped electrodes (see Fig. **2**). We investigated the following designs:

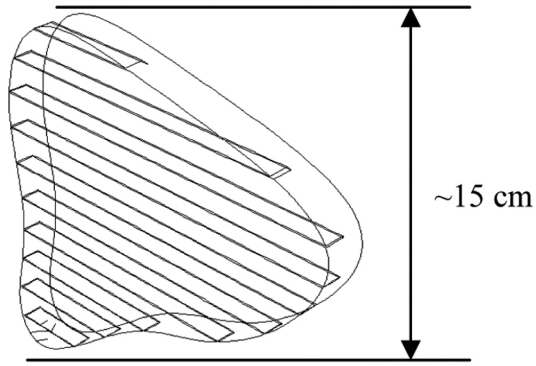

Fig. (3). Geometry for typical resection plane in the liver, with inserted blade electrode array (only part of the blades in the tissue are shown; actual electrodes extend beyond tissue).

Monopolar 6-Electrode Array

Monopolar application of RF energy (i.e. between the electrodes, and a dispersive electrode) is the standard method, but may have limitations for this application since little power is deposited between closely spaced electrodes [23], as in a multi-electrode array.

Bipolar 2-Electrode Array with Needle Electrodes

Bipolar voltage application preferentially heats tissue in-between electrodes, resulting in possibly higher tissue temperatures and improved performance in terms of vessel coagulation.

Bipolar voltage could be applied to a multi-electrode array with alternating poles (e.g. for 6 electrodes: +,–,+,–,+, –); however, that would not allow independent control of power for each electrode as is required to adjust for tissue thickness, local differences in perfusion, etc.

Bipolar 2-Electrode Array with Blade Electrodes

Blade electrodes cause more tissue damage during insertion but have more uniform power deposition between electrodes, and may provide higher temperatures in-between electrodes than with needle electrodes.

Effect of Electrode Spacing for Bipolar Electrode Arrays

Bipolar voltage application is most effective if electrodes are spaced very closely. With increasing electrode spacing the tapering of the coagulation zone in-between electrodes increases. We investigated different electrode distances to determine ideal spacing to create a coagulation zone of even thickness.

Rapid Switching of Bipolar Voltage for 6-Electrode Array

To extend bipolar voltage application from a 2-electrode array to multiple electrodes, we used rapid switching of

voltage application between adjacent electrodes. Power is applied for 1 s between electrodes 1 and 2, for 1 s between electrodes 2 and 3, and so on (see Fig. **4**). This method has the advantage of enabling control of deposited power between each pair by changing the time period of voltage application. Independent control of each pair is necessary to control power depending on tissue thickness, and vicinity to large vessels.

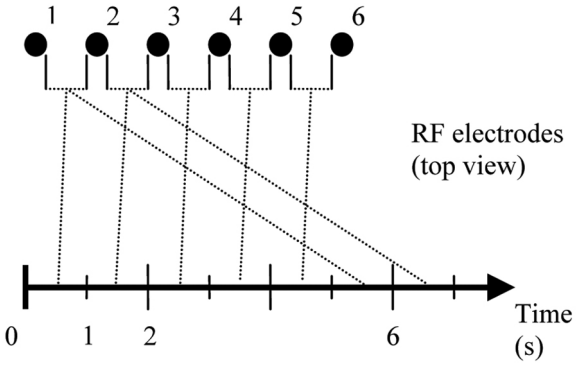

Fig. (4). Voltage is applied between adjacent electrode pairs and sequentially switched between different pairs in a round-robin fashion.

Material Properties

Healthy liver tissue was modeled with the tissue properties as shown in Table **1**. For electrical tissue conductivity, we used values from *in vivo* measurements since electrical conductivity changes rapidly when tissue is removed from the body [24]. Electrical conductivity was assumed to be temperature dependent, with a temperature coefficient of 1.5%/ºC [25]. At 100 ºC, vaporization occurs, gas forms, and an electrically insulating layer is created. To account for this phenomenon, a rapid linear drop in tissue conductivity by a factor of 10,000 between 100 ºC and 102 ºC was assumed, which limits any further power deposition by RF energy above boiling temperatures. In addition, a latent heat associated with water vaporization of 2,257 J/kg was assumed at 100 ºC.

Table 1. Tissue Properties

Electrical Conductivity	0.33 S/m at 37 °C
Density	1060 kg/m^3
Specific Heat	3600 J/(kg · K)
Thermal Conductivity	0.512 W/(m · K)

Joule Heating and the Bioheat Equation

Joule heating arises when the energy dissipated by an electric current flowing through a conductor is converted into thermal energy. The heating of liver tissue during radiofrequency ablation, and cooling due to blood perfusion is governed by the bioheat transfer equation [26].

$$\rho c \frac{\partial T}{\partial t} = \nabla \cdot k \nabla T + J \cdot E - h_{bl}(T - T_{bl}) \qquad (1)$$

$$h_{bl} = \rho_{bl} c_{bl} w_{bl}$$

where ρ is the density (kg/m^3), c is the specific heat (J/kg·K), k is the thermal conductivity (W/m·K), J is the current density (A/m^2) and E is the electric field intensity (V/m). T_{bl} is the temperature of blood, ρ_{bl} is the blood density (kg/m^3), c_{bl} is the specific heat of the blood (J/kg·K), and w_{bl} is the blood perfusion (ml/ml/s). h_{bl} is the convective heat transfer coefficient accounting for the blood perfusion. Electric field intensity E, and current density J are related by electrical conductivity σ according to (2).

$$J = E \cdot \sigma \qquad (2)$$

Blood Perfusion

To obtain results comparable to *in vivo* experiments, perfusion has to be included in the models. Perfusion was modeled according to the bioheat equation as a distributed heat sink. We assumed perfusion of 1 L/kg/min [25]. We further assumed cessation of perfusion once tissue was coagulated (i.e. above 60 ºC).

It is well known that tissue damage depends on both temperature and time [27]. However, previous studies have shown that for ablative therapies isotherms give reasonable estimates of tissue damage [28]. In this study we are interested in the region of tissue coagulation, which is smaller than the region where tissue damage occurs. Since protein coagulation occurs around 60 ºC [29], we used this temperature to estimate the boundary of the coagulation zone.

Model Geometry

The geometry of the electrode array is shown in Fig. (**1**) for an array of needle electrodes. Arrays were created of needle electrodes (1.2 mm diameter, 18 gauge), and blade shaped electrodes (5 × 0.1 mm rectangular cross section), (see Fig. **2**) at different distances. Distances between electrodes are measured from electrode centers. Since tissue thickness is large compared to electrode diameter, we can assume uniform power distribution and tissue temperature along the electrode axis, allowing us the use of 2-D models. The electrode arrays were placed centered into a tissue block of 100 × 200 mm cross-section, and RF frequency at 500 kHz was applied to the electrodes.

All models included blood perfusion until 60 ºC as described above. Initial tissue temperature was 37 ºC, which is human *in vivo* body temperature. Body temperature was also assigned to the model boundary as thermal boundary condition. Monopolar models were constructed by applying a ground potential to the outer boundary of the model and a positive potential to the electrode. Bipolar models were constructed by applying ground potential to one electrode and a positive potential to the neighbor electrode (see Fig. **4**). For all models we determined current density profile, and temperature profile for up to 3 min. Since the absolute current density changes according to applied potential, we show current density values relative to maximum current density. We terminated the simulations at 3 min, since no significant change in tissue temperature was observed after this time.

FEM modeling was conducted using the commercial FEM software package ABAQUS 6.3 (Hibbitt, Karlsson & Sorensen, Inc., Pawtucket, RI). ABAQUS/CAE was the

RESULTS

Monopolar 6-Electrode Array

Fig. (**6**) shows the cross-sectional temperature profile after 3 min for monopolar voltage application. Fig. (**7**) shows the corresponding current density profile. Temperature at the center between electrodes after 3 min was 52 ºC. Since all electrodes are at the same electric potential, little electric current flows between electrodes resulting in reduced temperatures in-between electrodes.

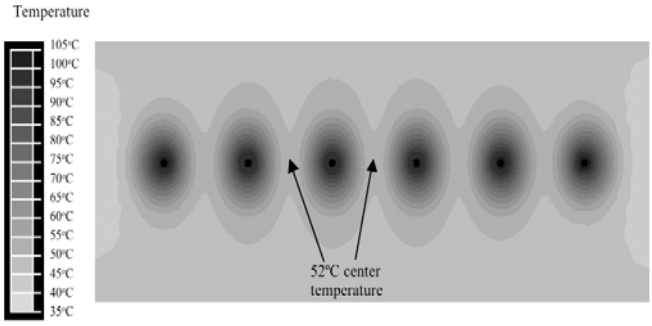

Fig. (6). Array of six needle electrodes at 1.5 cm distance, with voltage applied in monopolar mode (same voltage to all electrodes). Figure shows temperature contour at 3 min. Center temperature of 52 ºC (arrow) due to reduced inter-electrode heating.

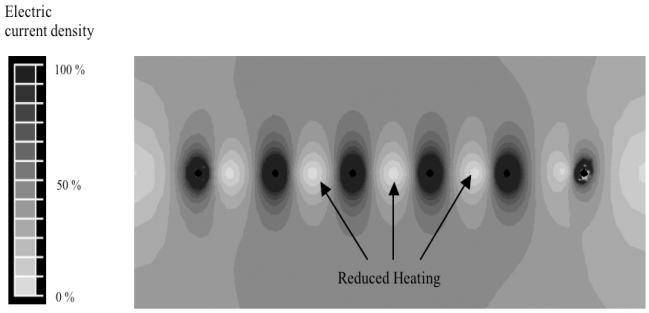

Fig. (7). Array of six needle electrodes at 1.5 cm distance, with voltage applied in monopolar mode (same voltage to all electrodes). Figure shows relative current density profile. Monopolar application results in reduced heating between electrodes (arrows) since electrodes are at same electrical potential.

Bipolar 2-Electrode Arrays

Figs. (**8** and **9**) show the cross-sectional temperature profile after 3 min bipolar voltage application for needle, and blade electrodes, respectively. Center temperature was 83 ºC for needle electrodes, and 97 ºC for blade electrodes.

lectrode Shape and Spacing with 2-Electrode Arrays

Needle and blade shaped electrode designs were compared at spacings of 1, 1.5, and 2 cm. Coagulation zone width was measured as the minimum diameter at the center point between electrodes corresponding to the 60 °C contour as demonstrated in Fig. (**5**). Results are summarized in Table **2**.

Rapid Switching with 6-Electrode Blade Array

Fig. (**11**) shows the temperature profile at 3 min. Temperatures close to 100 ºC are obtained throughout the tissue slice.

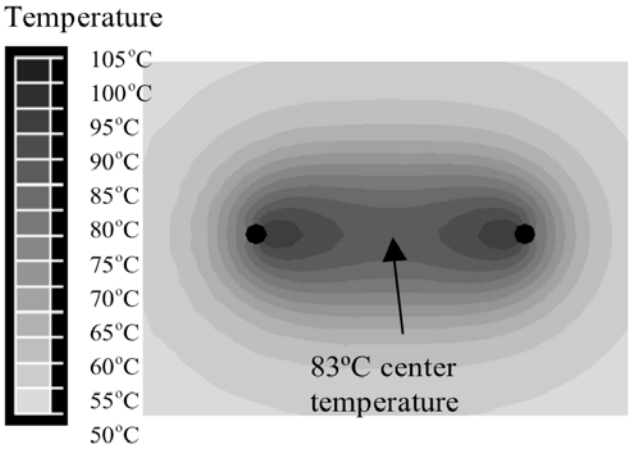

Fig. (8). Two needle electrodes at 1.5 cm distance, with voltage applied in bipolar mode (between electrodes). Figure shows temperature contour at 3 min.

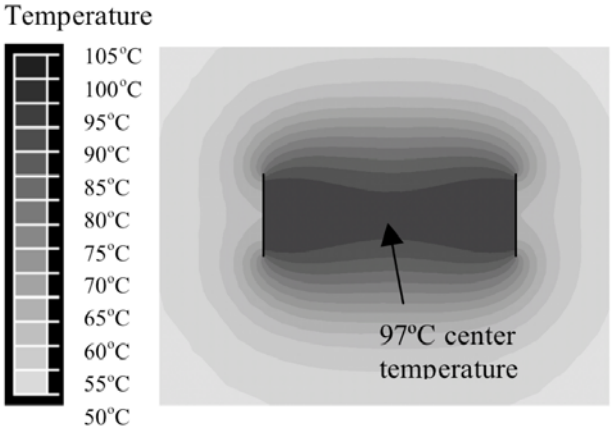

Fig. (9). Blade electrodes at 1.5 cm distance, with voltage applied in bipolar mode (between electrodes). Figure shows temperature contour at 3 min.

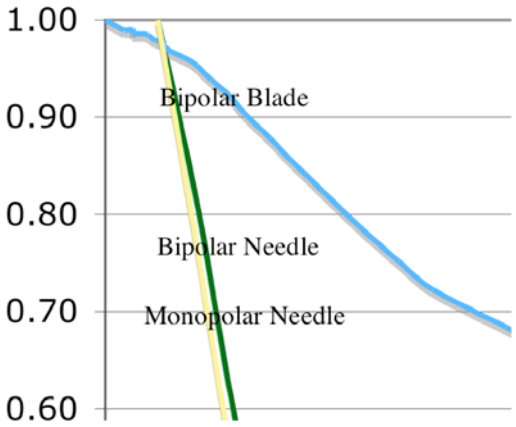

Fig. (10). Relative electric current density through center line between two electrodes (see Fig. **5**) 15 mm apart. Blade electrodes with bipolar voltage application deposit power throughout the slice, while bipolar needle, and monopolar needle electrodes only produce heat close to the electrodes. Note that due to different electrode size, surfaces of needle electrodes are at x = 0.6 and 14.4 mm, and surfaces of blade electrodes are at x = 0.05 and 4.95 mm.

Table 2. Center Temperature and Width of Coagulation Zone (Center Between Electrodes) for Different Electrode Shapes and Spacings in Bipolar Mode. Width is Measured as Shown in Fig. (5)

Probe	Spacing	60 seconds		180 seconds	
Type	cm	Temp. °C	Width mm	Temp. °C	Width mm
needle	1	87.6	7.7	91.4	9.7
needle	1.5	63.9	3.4	83.3	9.4
needle	2.0	51.0	0.0*	55.4	0.0*
blade	1.0	97.5	10.6	95.0	10.7
blade	1.5	94.5	12.0	93.5	13.2
blade	2.0	80.8	10.2	93.0	14.0

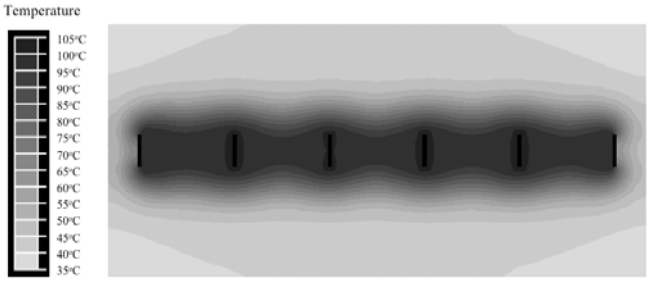

Fig. (11). Linear array of 6 blade electrodes at 1.5 cm distance. Voltage is rapidly switched between electrode pairs at 1 s intervals (see Fig. **4**). Coagulation zone is ~1.5 cm wide after 3 min.

DISCUSSION

Surgical liver resection is the current standard treatment for both primary and metastatic liver cancer; part of the liver (often one of the two liver lobes) is surgically removed. Unfortunately this operation is still associated with considerable blood loss. We present a new device to assist liver resection that can potentially significantly reduce inter-operative blood loss. The device consists of a linear array of electrodes (see Fig. **1**). The electrode array is inserted into the liver in the plane, where resection is intended (Fig. **3**), and the tissue plane is coagulated by application of RF energy. Then tissue can be cut along that plane with minimum blood loss. We estimate the necessary width of the coagulation zone for the resection plane to be 1 to 2 cm wide. A coagulation zone that is too wide unnecessarily destroys healthy liver tissue and creates the risk of damage to major vessels, while a coagulation zone of inadequate width could not be effectively transected. We employed FEM computer models to investigate different device designs.

In all models, we applied RF energy for 3 min since tissue temperature does not change significantly after this time. Initially, we investigated monopolar application of RF energy, where the RF voltage is applied between the electrode array and a ground pad. Since all electrodes are at same electric potential, little RF current is deposited in-between the electrodes (Fig. **7**). The result is comparably low tissue heating, with a center temperature of 52 ºC between electrodes; this temperature is insufficient to provide tissue coagulation (Fig. **6**). When RF energy is applied bipolar between two needle electrodes at same distance as in the monopolar case, much higher tissue temperatures are obtained (Fig. **8**) since RF current now flows in-between the electrodes; center temperature was 83 ºC in this case. Note that in Fig. (**8**) only two electrodes are considered; bipolar power application however can be extended to more than 2 electrodes by rapid switching (Fig. **4**) as discussed later.

Apart from needle electrodes, we also investigated blade shaped electrodes (Fig. **2**) for bipolar energy application. RF current flow between two large parallel plates and resulting heating pattern are uniform, and two parallel plate electrodes approximate this situation better than needle electrodes. Fig. (**9**) shows the resulting temperature profile when blade electrodes are used. Notice that tissue temperature is above 95 ºC throughout much of the slice, with center temperature of 97 ºC. Fig. (**10**) compares the current density through the center line (dotted line in Fig. **5**) for monopolar needle, bipolar needle, and bipolar blade electrodes. For monopolar needle electrodes, current density drops rapidly with increasing distance from the electrode. Bipolar application of RF energy improves the current density profile, and the use of blade electrodes in bipolar mode results in significant further improvement. With blade electrodes, a very uniform current density profile is obtained where all tissue within the slice is directly heated by RF energy.

Currently clinically used RF devices employ the monopolar method, and are not able to coagulate vessels larger than 3 mm diameter [22]. This limitation is largely due to the fact that the power deposition around the electrode drops rapidly (deposited power around needle electrode is $\sim 1/r^2$, r = electrode radius). Significant direct heating by RF energy only occurs within a few mm from the electrode for current commercial devices, and most of the coagulation zone is created by thermal conduction from the hot regions next to the electrode. Since it is difficult to coagulate a vessel by thermal conduction from outside while the vessel is cooled by blood flow from the inside, current RF devices can only coagulate small vessels. Two-electrode arrays with closely spaced needle electrodes, and especially with blade electrodes and bipolar voltage application have a current density profile where significant power is deposited throughout the tissue slice (see Fig. **10**). Any vessels in this slice are heated directly by RF energy, and not merely by thermal conduction. This should facilitate coagulation of larger vessels than possible with current devices. In addition, the bipolar voltage application eliminates the need for a

ground pad. A ground pad limits the amount of power that can be applied to the tissue because of the danger of ground pad skin burns when too much power is used [32]. Current RF devices use up to 200 W power, but we estimate the device described here will require up to 500 W for rapid coagulation of a tissue slice, increasing the risk of ground pad burns. Bipolar voltage application requires electrodes to be parallel for uniform heating between electrodes. Thus a template with rigid control of the distance between electrodes is essential.

We investigated 2-electrode arrays with different electrode distances for needle and blade electrodes with bipolar power application to determine the ideal distance. The distance should be close enough to create a coagulation plane without much tapering between electrodes; the closer the spacing, the more electrodes are required which is undesirable since it makes the usage more complex. We found a spacing of 1.5 cm with blade electrodes to create a coagulation slice of desired width. Whether this electrode configuration is sufficient to coagulate all large vessels in a typical resection plane will have to be determined experimentally. If large vessels cannot be coagulated, an option is to occlude liver inflow to reduce convective cooling. Inflow occlusion is routinely performed during liver resection to reduce blood loss, and can be performed for up to 25 min.

To extend the method of bipolar voltage application from two electrodes to an array of multiple electrodes, we use rapid switching where RF voltage is applied for brief time periods to adjacent electrode pairs. Power is applied to electrodes 1+2 for a brief period (1 s in our models), then to electrodes 2+3, and so on (see Fig. **4**). This way we are able to rapidly heat a slice of tissue applying voltage bipolar to all electrodes in the array. Fig. (**11**) shows that the temperature profile is very uniform with high tissue temperatures close to 100 ºC throughout the slice. In our models we were able to obtain a uniform coagulation slice ~1.5 cm wide within 3 min of application time.

One major risk of this device may be inadvertent damage to critical structures such as the biliary system and the vena cava, which may limit application of the electrode array close to these structures.

CONCLUSIONS

We investigated a linear electrode array for potential application to coagulating a tissue slice for assisting liver resection. We found an array of blade electrodes with RF energy applied between adjacent electrodes and rapid switching between multiple electrode pairs to be superior to using the same method with needle electrodes. Voltage application between adjacent electrodes is superior to monopolar voltage application (i.e. to all electrodes). RF energy is deposited uniformly between the blade electrodes, resulting in high tissue temperatures close to 100 ºC throughout the slice. This configuration produces a ~1.5 cm wide plane of coagulated tissue and may allow for large vessel coagulation.

This work was supported by the National Institutes of Health, Grants Number R01DK58839, R01CA118990, and Number C06 RR018823 from the Extramural Research Facilities Program of the National Center for Research Resources.

REFERENCES

[1] K. Hanazaki, S. Kajikawa, N. Shimozawa, K. Shimada, M. Hiraguri, N. Koide, W. Adachi, and J. Amano, "Hepatic resection for large hepatocellular carcinoma," *Am. J. Surg.*, vol. 181, pp. 347-53, Apr 2001.

[2] K. E. Harmon, J. A. Ryan, Jr., T. R. Biehl, and F. T. Lee, "Benefits and safety of hepatic resection for colorectal metastases," *Am. J. Surg.*, vol. 177, pp. 402-4, May 1999.

[3] A. Jemal, R. Siegel, E. Ward, T. Murray, J. Xu, and M. J. Thun, "Cancer statistics, 2007," *CA Cancer J. Clin.*, vol. 57, pp. 43-66, Jan-Feb 2007.

[4] A. R. Sasson, and E. R. Sigurdson, "Surgical treatment of liver metastases," *Semin. Oncol.*, vol. 29, pp. 107-18, Apr 2002.

[5] J. F. Buell, A. Koffron, A. Yoshida, M. Hanaway, A. Lo, R. Layman, D. C. Cronin, M. C. Posner, and J. M. Millis, "Is any method of vascular control superior in hepatic resection of metastatic cancers? Longmire clamping, pringle maneuver, and total vascular isolation," *Arch. Surg.*, vol. 136, pp. 569-75, May 2001.

[6] M. Rees, G. Plant, J. Wells, and S. Bygrave, "One hundred and fifty hepatic resections: evolution of technique towards bloodless surgery," *Br. J. Surg.*, vol. 83, pp. 1526-9, Nov 1996.

[7] X. D. Zhou, Z. Y. Tang, Y. Q. Yu, Z. C. Ma, D. B. Xu, Y. X. Zheng, and B. H. Zhang, "Microwave surgery in the treatment of hepatocellular carcinoma," *Semin. Surg. Oncol.*, vol. 9, pp. 318-22, Jul-Aug 1993.

[8] N. Taniai, M. Onda, T. Tajiri, K. Akimaru, H. Yoshida, and Y. Mamada, "Hepatic parenchymal resection using an ultrasonic surgical aspirator with electrosurgical coagulation," *Hepatogastroenterology*, vol. 49, pp. 1649-51, Nov-Dec 2002.

[9] J. Melendez, E. Ferri, M. Zwillman, M. Fischer, R. DeMatteo, D. Leung, W. Jarnagin, Y. Fong, and L. H. Blumgart, "Extended hepatic resection: a 6-year retrospective study of risk factors for perioperative mortality," *J. Am. Coll. Surg.*, vol. 192, pp. 47-53, Jan 2001.

[10] W. R. Jarnagin, M. Gonen, Y. Fong, R. P. DeMatteo, L. Ben-Porat, S. Little, C. Corvera, S. Weber, and L. H. Blumgart, "Improvement in perioperative outcome after hepatic resection: analysis of 1,803 consecutive cases over the past decade," *Ann. Surg.*, vol. 236, pp. 397-406; discussion 406-7, Oct 2002.

[11] N. Nagasue, T. Ono, A. Yamanoi, H. Kohno, O. N. El-Assal, H. Taniura, and M. Uchida, "Prognostic factors and survival after hepatic resection for hepatocellular carcinoma without cirrhosis," *Br. J. Surg.*, vol. 88, pp. 515-22, Apr 2001.

[12] T. Nonami, A. Nakao, T. Kurokawa, H. Inagaki, Y. Matsushita, J. Sakamoto, and H. Takagi, "Blood loss and ICG clearance as best prognostic markers of post-hepatectomy liver failure," *Hepatogastroenterology*, vol. 46, pp. 1669-72, May-Jun 1999.

[13] M. Shimada, K. Takenaka, Y. Fujiwara, T. Gion, K. Shirabe, K. Yanaga, and K. Sugimachi, "Risk factors linked to postoperative morbidity in patients with hepatocellular carcinoma," *Br. J. Surg.*, vol. 85, pp. 195-8, Feb 1998.

[14] C. C. Wu, S. M. Kang, W. M. Ho, J. S. Tang, D. C. Yeh, T. J. Liu, and K. P'Eng F, "Prediction and limitation of hepatic tumor resection without blood transfusion in cirrhotic patients," *Arch. Surg.*, vol. 133, pp. 1007-10, Sep 1998.

[15] G. Gozzetti, A. Mazziotti, G. L. Grazi, E. Jovine, A. Gallucci, S. Gruttadauria, A. Frena, M. Morganti, G. Ercolani, M. Masetti, and F. Pierangeli, "Liver resection without blood transfusion," *Br. J. Surg.*, vol. 82, pp. 1105-10, Aug 1995.

[16] G. G. Jamieson, L. Corbel, J. P. Campion, and B. Launois, "Major liver resection without a blood transfusion: is it a realistic objective?," *Surgery*, vol. 112, pp. 32-6, Jul 1992.

[17] D. A. Kooby, J. Stockman, L. Ben-Porat, M. Gonen, W. R. Jarnagin, R. P. Dematteo, S. Tuorto, D. Wuest, L. H. Blumgart, and Y. Fong, "Influence of transfusions on perioperative and long-term outcome in patients following hepatic resection for colorectal metastases," *Ann. Surg.*, vol. 237, pp. 860-9; discussion 869-70, Jun 2003.

[18] R. Pellicci, M. Pasqualini, M. Stella, and A. Percivale, "Radiofrequency Assisted Liver Resection: A New Technical Device," *J. Gastrointest. Surg.*, vol. 7, p. 279, 2003.

[19] K. Tabuse, M. Katsumi, Y. Kobayashi, H. Noguchi, H. Egawa, O. Aoyama, H. Kim, Y. Nagai, H. Yamaue, K. Mori, Y. Azuma, and T. Tsuji, "Microwave surgery: hepatectomy using a microwave tissue coagulator," *World J. Surg.*, vol. 9, pp. 136-43, Feb 1985.

[20] J. C. Weber, G. Navarra, N. A. Habib, P. Bachellier, and D. Jaeck, "Laparoscopic radiofrequency-assisted liver resection," *Surg. Endosc.*, vol. 17, p. 834, May 2003.

[21] J. C. Weber, G. Navarra, L. R. Jiao, J. P. Nicholls, S. L. Jensen, and N. A. Habib, "New technique for liver resection using heat coagulative necrosis," *Ann. Surg.*, vol. 236, pp. 560-3, Nov 2002.

[22] D. S. Lu, S. S. Raman, D. J. Vodopich, M. Wang, J. Sayre, and C. Lassman, "Effect of vessel size on creation of hepatic radiofrequency lesions in pigs: assessment of the "heat sink" effect," AJR. *Am. J. Roentgenol.*, vol. 178, pp. 47-51, 2002.

[23] D. Haemmerich, S. Tungjitkusolmun, S. T. Staelin, F. T. Lee, Jr., D. M. Mahvi, and J. G. Webster, "Finite-element analysis of hepatic multiple probe radio-frequency ablation," *IEEE Trans. Biomed. Eng.*, vol. 49, pp. 836-42, Aug 2002.

[24] D. Haemmerich, O. R. Ozkan, J. Z. Tsai, S. T. Staelin, S. Tungjitkusolmun, D. M. Mahvi, and J. G. Webster, "Changes in electrical resistivity of swine liver after occlusion and postmortem," *Med. Biol. Eng. Comput.*, vol. 40, pp. 29-33, Jan 2002.

[25] F. A. Duck, *Physical Properties of Tissue*. London: Academic Press, 1990.

[26] H. H. Pennes, "Analysis of tissue and arterial blood temperatures in the resting human forearm," *J. Appl. Physiol.*, vol. 1, pp. 93-122, 1948.

[27] S. A. Sapareto, and W. C. Dewey, "Thermal dose determination in cancer therapy," *Int. J. Radiat. Oncol. Biol. Phys.*, vol. 10, pp. 787-800, Jun 1984.

[28] S. J. Graham, L. Chen, M. Leitch, R. D. Peters, M. J. Bronskill, F. S. Foster, R. M. Henkelman, and D. B. Plewes, "Quantifying tissue damage due to focused ultrasound heating observed by MRI," *Magn. Reson. Med.*, vol. 41, pp. 321-8, Feb 1999.

[29] M. D. Sherar, J. A. Moriarty, M. C. Kolios, J. C. Chen, R. D. Peters, L. C. Ang, R. S. Hinks, R. M. Henkelman, M. J. Bronskill, and W. Kucharcyk, "Comparison of thermal damage calculated using magnetic resonance thermometry, with magnetic resonance imaging post-treatment and histology, after interstitial microwave thermal therapy of rabbit brain," *Phys. Med. Biol.*, vol. 45, pp. 3563-76, Dec 2000.

[30] D. Haemmerich, and J. G. Webster, "Automatic control of finite element models for temperature-controlled radiofrequency ablation," *Biomed. Eng. Online.*, vol. 4, pp. 1-8, 2005.

[31] F. T. Lee, Jr., D. Haemmerich, A. S. Wright, D. M. Mahvi, L. A. Sampson, and J. G. Webster, "Multiple probe radiofrequency ablation: pilot study in an animal model," *J. Vasc. Interv. Radiol.*, vol. 14, pp. 1437-42, Nov 2003.

[32] S. N. Goldberg, L. Solbiati, E. F. Halpern, and G. S. Gazelle, "Variables affecting proper system grounding for radiofrequency ablation in an animal model," *J. Vasc. Interv. Radiol.*, vol. 11, pp. 1069-75, Sep 2000.

Received: September 03, 2009 Revised: November 10, 2009 Accepted: December 20, 2009